ARTICLE

OBC
www.rsc.org/obc

Crystal structures and properties of mutagenic *N*-acyloxy-*N*-alkoxyamides — "most pyramidal" acyclic amides

Ashley-Mae E. Gillson,[a] Stephen A. Glover,*[a] David J. Tucker[a] and Peter Turner[b]
[a] *Division of Chemistry, School of Biological, Biomedical and Molecular Sciences, University of New England, Armidale 2351, New South Wales, Australia*
[b] *School of Chemistry, University of Sydney, Sydney 2006, New South Wales, Australia*

Received 29th May 2003, Accepted 31st July 2003
First published as an Advance Article on the web 27th August 2003

X-Ray data for two *N*-acyloxy-*N*-alkoxyamides, a class of direct-acting mutagens, indicate extreme pyramidalisation at the amide nitrogen in keeping with spectroscopic and theoretically determined properties of amides with bisoxo-substitution at nitrogen. The combined electronegativity of two oxygens leads to average angles at nitrogen of 107.8 and 108.1° and $|\chi_N|$ of 66° and 65°. The sp^3 nature of nitrogen results in negligible amide resonance as evidenced by long *N–C(O)* bonds, high IR carbonyl stretch frequencies, carbonyl ^{13}C NMR data and very low amide isomerisation barriers. In addition, conformations in the solid state support a strong n_O–σ^*_{NOAc} anomeric interaction as predicted by molecular orbital theory. HF/6-31G* calculations on formamide, *N*-methoxyformamide and *N*-formyloxy-*N*-methoxyformamide support these findings.

Introduction

The nitrogen atom of normal amides is almost always planar or close to planar and has a p-type lone pair of electrons that is loosely bound and therefore interacts strongly with the carbonyl, principally through pi overlap with the carbonyl carbon.[1] This process creates a partial double bond (typically around 132–137 pm long) between the amide nitrogen and the carbon which is strengthened, additionally, by sigma donation from carbon to the nitrogen. Both effects result in severely restricted rotation about this bond since this process removes pi overlap and reduces the electronegativity of the nitrogen, which becomes sp^3 hybridised and less electron-withdrawing in the orthogonal form. Thus normal amide linkages are both planar, or nearly so, and undergo *E–Z* isomerisation relatively slowly with a $\Delta G^{\ddagger}$ of between 70 and 90 kJ mol^{-1}.[2–4] To a large degree, lone pair resonance accounts for the chemistry of amides which are far less readily hydrolysed or reduced when compared to say esters.[4] In addition, although there is often a small distortion from coplanarity, many of the properties of polypeptides, simple and complex proteins relate to their tertiary structure, which is a function of the amide connecting units. The idea that amide linkages might be without these properties is a relatively new one.

Recently there has been a good deal of interest in "twisted amides", amides in which the carbonyl orientation is significantly rotated about the R_2N–*C(O)* bond and in which resonance delocalisation of the nitrogen lone pair is partially or completely lost.[4–14] Such amides can act as acylating agents, are more basic than planar amides and behave as both amines and ketones or aldehydes.[6,8,10,15–18] Twisted amides form in situations where the amide nitrogen is incorporated into a rigid or semi-rigid ring structure best accommodated by sp^3 hybridised nitrogen.[6,8–10,14,19] Such hybridisation is not conducive to both lone pair orbital overlap with the carbonyl carbon and sigma acceptance from that carbon and, as a consequence, these amides have long *N–C(O)* bonds and high IR stretch frequencies more appropriate to ketones or aldehydes. In certain substances, twisting about *N–C(O)* bonds is brought about by steric constraints.[6,7,11,12,15,20,21] Such amides exhibit similar carbonyl characteristics to those above, although pyramidalisation at nitrogen is not a prerequisite.

As a spin-off from our extensive research on formation and reactions of *N*-alkoxynitrenium ions[22–24] and subsequently on synthesis, reactions and biological properties of mutagenic *N*-acetoxy-*N*-alkoxybenzamides,[25–33] we have discovered that amides, geminally substituted at nitrogen with two electronegative heteroatoms (Fig. 1a) display vastly different properties when compared to normal amides. To maximize electron density distribution near the electronegative atoms, such amides possess tetrahedral nitrogens without their incorporation into a restraining configuration and the lone pair gains s character and is in an sp^3 hybrid orbital. As a consequence, these too have very little lone pair delocalisation onto the carbonyl. They have reduced *N–CO* double bond character and low barriers to rotation about the amide linkage. Collectively, *N*,*N*-bisheteroatom-substituted amides exhibit high carbonyl stretch frequencies (1730–1750 cm^{-1}) and time-averaging of *E–Z* conformations in their NMR spectra.[34,35]

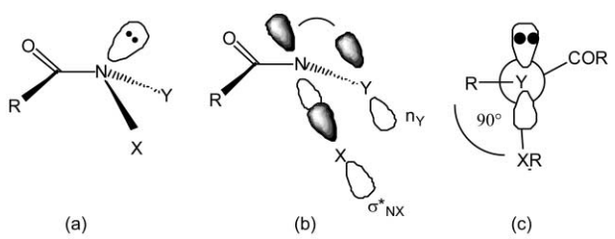

Fig. 1 (a) Pyramidal structure, (b) anomeric interaction and (c) conformation about the *N*–Y bond in anomeric amides.

Theoretical calculations have supported our spectroscopic findings.[36–38] Calculations on the *ONO* system *N*,*N*-dimethoxyformamide (**1**), the *ONCl* system *N*-chloro-*N*-methoxyformamide (**2**) and *NNCl* system *N*-chloro-*N*-dimethylaminoformamide (**3**) all predict a strong degree of pyramidalisation at nitrogen (average angles between 112° and 115°), together with longer than normal *N–C(O)* bonds (139.6–141.8 pm). Calculated barriers to *E–Z* isomerisation are reduced to between 25 and 42 kJ mol^{-1}.[36] The *NNO* system, *N*-methoxy-*N*-dimethylaminoformamide (**4**) exhibited properties somewhere between **1**–**3** and normal amides (*E–Z* isomerisation barrier of 53 kJ mol^{-1}; *N–C(O)* bond length 138.5 pm; average angle at nitrogen of 116°) as a consequence of the net reduced electronegativity of the nitrogen/oxygen substituents.[37] Nitrogen inversion barriers are low in all four configurations (10.5 kJ

DOI: 10.1039/b306098p

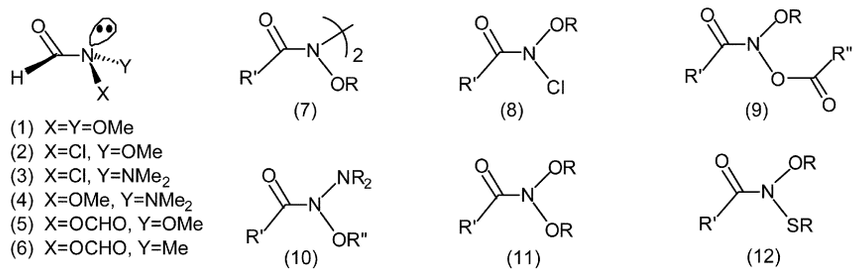

mol^{-1}) on account of resonance delocalisation in the planar transition state for this isomerisation process.

In addition, calculations predict strong n_Y–σ^*_{NX} anomeric effects between nitrogen substituents (Fig. 1b).[36,37] In the case of *NNCl* and *NNO* systems **3** and **4**, this negative hyperconjugation gives rise to very significant *N*–*N* rotation barriers of 81 and 60 kJ mol^{-1} respectively. Where oxygen lone pairs are involved (*ONO* and *ONCl* systems **1** and **2**), the analogous *N*–*O* rotation barrier is reduced to about 45 kJ mol^{-1}. In all cases, ground-state conformations in which there is optimum overlap between the p-type lone pair on the donor heteroatom, n_Y, and the σ^*_{NX} orbital (Fig. 1c) are preferred. For these reasons, we have called bisheteroatom-substituted amides "anomeric amides".[34]

While some such amides have been made before by other groups (hydrazines (**7**),[39–42] *N*-alkoxy-*N*-chloroamides (**8**)[43–45]), they have not emphasised or exploited their unusual properties. However, we have verified, spectroscopically, many of these theoretical properties and have discovered new chemistry of *NNO* (**7** and **10**),[28,31,35,46,47] *ONO* (**9** and **11**),[27–31,48,49] *ONCl* (**8**)[25,38,49] and *ONS* (**12**)[48,50] systems. Recently we published the crystal structure of the symmetrically substituted hydrazine **13**, which exhibits strong pyramidalisation at both nitrogens and other properties in confirmation of the theoretical predictions for *NNO* systems.[35] In this paper, we report the structures of two *N*-acyloxy-*N*-alkoxyamides **17** and **18**, both of which are *ONO* systems in which the effective electronegativity of one oxygen atom attached to nitrogen is enhanced by acylation and these confirm structural features outlined above. Recently Kirby reported the "most twisted" amide **14** in which the nitrogen is incorporated into the bridgehead position of 2-adamantanone.[8–10,51] Compounds **17** and **18** represent the "most pyramidal" acyclic amides synthesised to date.

Results and discussion

N-acyloxy-*N*-alkoxyamides **17** and **18** were synthesised as a part of our investigations into steric factors affecting the activity of this class of direct-acting mutagens.[27,29,30,32,33] In line with the protocol for the formation of a wide range of substrates (**9**), **17** and **18** were made by benzoyloxylation of the *N*-chlorinated hydroxamic esters, *N*-(4-*tert*-butylbenzyloxy)-benzamide (**15**) and *N*-(4-*tert*-butylbenzyloxy)-4-*tert*-butylbenzamide (**16**) with either sodium benzoate or sodium 4-*tert*-butylbenzoate in anhydrous acetone (Scheme 1).[27,30] Upon purification by centrifugal chromatography, this class of mutagens normally gives oils but, in these cases, solids were obtained which crystallised from ethyl acetate–petroleum spirit Single crystals of **17** and **18** suitable for X-ray diffraction analysis were accordingly obtained, and resultant ORTEP[52] depictions are presented in Figs. 2 and 3. Pertinent structural and spectroscopic features are provided in Table 1 together with corresponding data for the theoretical model, *N*-formyloxy-*N*-methoxyformamide (**5**), hydrazine **13** and Kirby's "most twisted" amide **14**.

Twist and pyramidal indices τ, χ_C and χ_N are in accordance with the Winkler–Dunitz system[19,53] for which defining geometrical parameters are illustrated in Fig. 4.

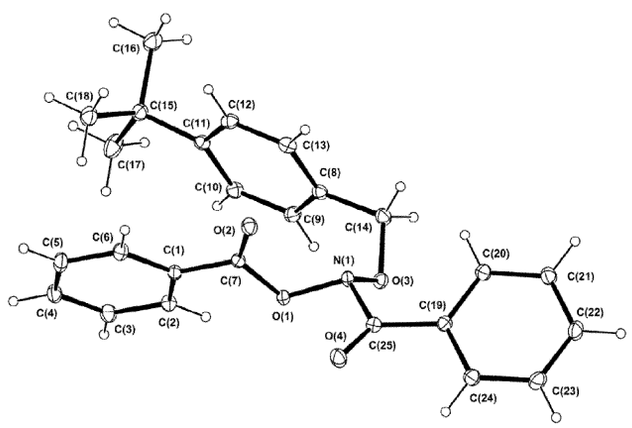

Fig. 2 ORTEP[52] depiction of *N*-benzoyloxy-*N*-(4-*tert*-butylbenzyloxy)benzamide (**17**) with displacement ellipsoids shown at the 20% level.

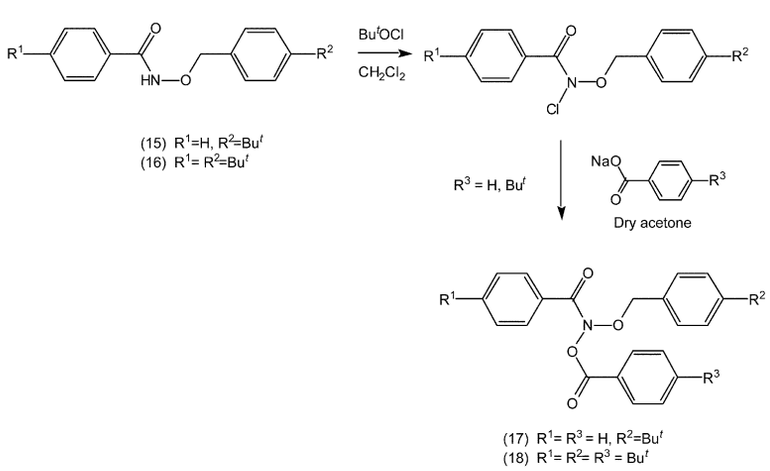

Scheme 1

Table 1 Selected structural and spectroscopic properties of *N*-acyloxy-*N*-alkoxyamides **17** and **18**, hydrazine **13**, 1-aza-2-adamantanone **14** and theoretical model **5**

				13		
Parameter[a]	**17**	**18**	**5**[e]	N1	N2	**14**
r_{CO}/pm	120.70	120.52	117.70	121.30	120.70	121.00
r_{CN}/pm	144.14	143.94	141.10	141.20	141.00	145.50
r_{NOR}/pm	140.17	140.14	136.10	140.30	141.10	—
r_{NOAcyl}/pm	143.96	144.14	137.50	138.90[f]		—
β_1/°	110.60	109.40	109.9	117.32	116.71	109.00
β_2/°	109.00	108.59	111.3	116.57	111.23	109.00
β_3/°	104.52	105.48	108.60	109.47	113.25	110.00
$\Sigma\beta$/°	324.14	323.51	329.8	343.36	341.19	328.00
δ/°[b]	35.86	36.49	30.2	16.64	18.81	32.00
$<\beta>$/°[c]	108.05	107.84	109.9	114.45	113.73	109.33
ω_1/°	49.25	50.36	−31.6	−36.00	−38.80	−60.00
ω_2/°	−21.39	−19.34	32.6	19.03	16.10	−120.00
ω_3/°	−135.77	−134.01	152.9	151.70	147.20	120.00
ω_4/°	163.63	165.03	−151.9	−168.70	−169.88	60.00
τ/°[d]	13.93	15.51	0.50	−8.49	−11.35	−90.00
χ_C/°[d]	5.02	4.37	−4.50	−7.70	−6.00	0.00
χ_N/°[d]	−65.62	−65.33	59.70	47.33	48.90	−60.00
ν_{max}/cm^{-1}	1730	1726		1711[g]		1732
δ^{13}C	174.2	174.2		168.7		200

[a] See Fig. 4 for definition of angles. [b] $\delta = 360 - \Sigma\beta$ [c] $<\beta> = \Sigma(\beta)/3$ [d] Amide distortion parameters defined in accordance with Winkler–Dunitz.[19,53] [e] Geometry calculated at HF/6-31G* level of theory. [f] *N–N* bond distance. [g] Degenerate carbonyl absorptions.

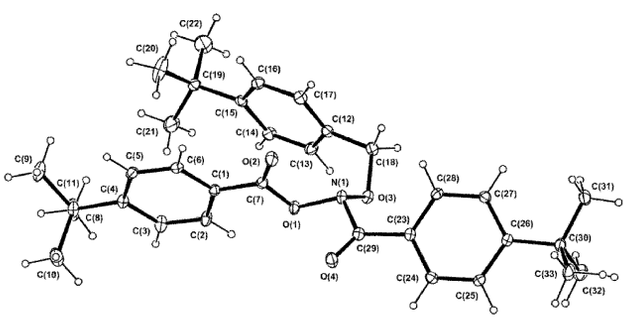

Fig. 3 ORTEP[52] diagram of *N*-(4-*tert*-butylbenzoyloxy-*N*-(4-*tert*-butylbenzyloxy)-4-*tert*-butylbenzamide (**18**) with displacement ellipsoids shown at the 20% level.

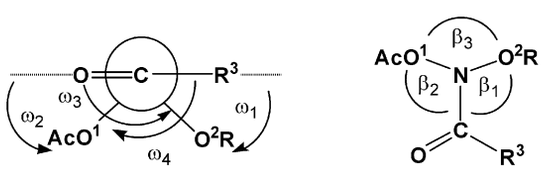

$$\tau = 1/2(\omega 1 + \omega 2)$$
$$\chi_C = (\omega_1 - \omega_3 + \pi) = (\omega_4 - \omega_2 + \pi)$$
$$\chi_N = (\omega_2 - \omega_3 + \pi) = (\omega_4 - \omega_1 + \pi)$$

Fig. 4 Winkler–Dunitz parameters for defining twist and pyramidality in amides.

Pyramidality at nitrogen

N-Acyloxy-*N*-alkoxyamides **17** and **18** are strongly pyramidal at nitrogen with $|\chi_N|$ values of well over 60° and average angles at nitrogen below that required by pure tetrahedral geometry as exemplified by the tetrahedral nitrogen in 1-aza-2-adamantanone (**14**) (Table 1). The geometrical distortion at nitrogen is consistent with trends in theoretical predictions of B3LYP/6-31G* which show average angles decreasing in the order *NNO* > *ONO* ~ *ONCl* > *NNCl* systems.[36,37] Recent calculations on *N*-formyloxy-*N*-methoxyformamide (**5**) at the HF/6-31G* level predicted an average angle at nitrogen of 109.9°.[50] In the same study, *N*-formyloxy-*N*-methylformamide (**6**) was far less

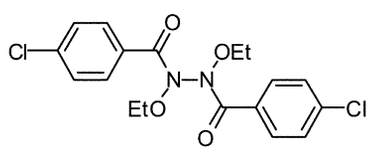

(13)

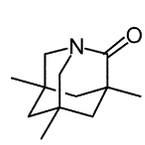

(14)

pyramidal at nitrogen (average angle of 116°) and the extreme pyramidality at nitrogen must be attributed to the presence on nitrogen of two electronegative oxygen atoms. Furthermore, from the X-ray structural data for **17** and **18**, as well as the theoretical comparisons for *N,N*-dimethoxyformamide (**1**)[36] and *N*-formyloxy-*N*-methoxyformamide (**6**),[50] *O*-acylation clearly results in even greater pyramidalisation at nitrogen. In addition, the degree of pyramidality (Table 1) is greater in **17** and **18** than at either nitrogen of the symmetrical hydrazine **13**[35] which reflects the lower net combined electronegativity of substituents at nitrogen in this system.

Analysis of the Cambridge Structural Database[54] showed that there are no *acyclic* tertiary amides (nitrogen not incorporated into a ring structure) with average angles at nitrogen less than 112°. Fig. 5(a) indicates that of the 1552 entries, average angles at nitrogen in all cases fall above 112° and **17** and **18** represent the "most pyramidal" acyclic tertiary amides discovered to date. In addition, the role of electronegative substituents in pyramidalisation of amides is reinforced by the fact that all but one of seven tertiary amide entries below 116° are either hydroxamic esters or hydroxamic acids. † Of 5382 primary, secondary and tertiary acyclic amide entries in the database, only 17 have angles smaller than 109° and all of these have *N–H* bonds. The apparent pyramidality in these few cases appears to be a consequence of errors in the placement of the hydrogen atoms in the structure model.

Twist angle

Both **17** and **18** also exhibit a significant degree of twisting around the *N–C(O)* bond (τ = 13.9 and 15.5° respectively). The

† One entry is an *N,N*-dimethyl urea. Pyramidalisation at one urea nitrogen is likely a result of reduced demand for amide delocalisation.

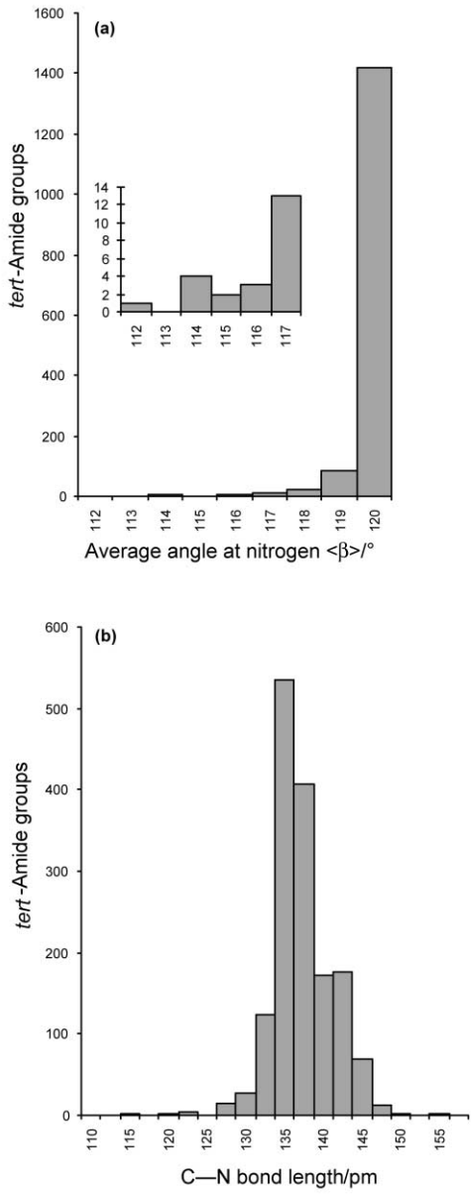

Fig. 5 (a) Average angles at nitrogen and (b) *N–C(O)* bond lengths from 1552 acyclic, tertiary amides in the Cambridge Structural Database, CSD 5.24.

barrier to *E–Z* isomerisation in *N*-acyloxy-*N*-alkoxyamides has been estimated to be below 30 kJ mol^{-1} [34] in line with the theoretical barrier for **5** (23.5 and 28.6 kJ mol^{-1} [50]). Since the lone pair on nitrogen resides in an sp^3 hybrid orbital, twisting angles in **17** and **18** are likely to arise from steric interactions or crystal packing rather than pi-orbital overlap considerations.

Amide bond lengths

The *N–C(O)* bonds (r_{C-N}, Table 1) are long when compared with normal, acyclic amides in the CSD (average bond length of 135.9 pm, median 135.3 pm). In the database, *N–C(O)* bonds show greater variability than the average bond angles but fewer than a hundred amides out of 1552 have similar or longer *N–C(O)* bonds (Fig. 5b) and in all of these, deviation from sp^3 hybridisation is minimal (<β> > 117°). Although *N–C(O)* bonds of *N*-acyloxy-*N*-alkoxyamides **17** and **18** cannot be compared directly with tertiary *N,N*-dialkylamides, they are only slightly shorter than the corresponding bond in the fully twisted lactam 1-aza-2-adamantanone (**14**) even though the twist angle is relatively small (Table 1). They are significantly longer than the amide bonds in the hydrazine **13** where *E–Z* isomerisation barriers were of the order of 54 kJ mol^{-1}.[35]

Table 2 Characteristic carbonyl vibrational frequencies for various anomeric amides[34]

Class		$\nu_{C=O}$/cm^{-1} ($CHCl_3$)
7		1700–1722
8		1717–1727
9	R″ = Me	1720–1730
	R″ = Aryl	1718–1735
11		1705–1715

The carbonyl bond length is similar in **17**, **18**, 1-aza-2-adamantanone **14** and the hydrazine **13** despite the different degrees of lone pair resonance (Table 1). Density functional calculations on **1**–**5** support this.[36,37,50] This is consistent with the carbonyl bond lengths in twisted amides, which are relatively insensitive to the degree of lone pair resonance. Kirby has attributed this to a negative hyperconjugative effect involving an n_O–σ^*_{CN} interaction impacting in an opposite sense upon the *C=O* bond length[9] but, based on Frontier Molecular Orbital concepts, Wiberg has suggested that transfer of pi density to the carbonyl carbon is the main process and oxygen gains relatively little electron density.[1] Similar arguments can account for the relative insensitivity of *C=O* bonds to loss of pi overlap in anomeric amides.

Spectroscopic properties

In contrast to *C=O* bond lengths, *C=O* vibrational frequencies are very sensitive to the extent of lone pair resonance in amides. In particular, increasing combined electronegativity of substituents at nitrogen results in a marked increase in the $\nu_{C=O}$ values.[34] Typical ranges for *C=O* stretch frequencies of anomeric amides are presented in Table 2. In accord with the increased electron-withdrawing effect of the ester carbonyl, *N*-acyloxy-*N*-alkoxyamides (**9**) absorb at a significantly greater $\nu_{C=O}$ than the *N,N*-dialkoxyamides (**11**). In general, we have found that electron-withdrawing substituents on both nitrogen substituents result in a $\nu_{C=O}$ at the higher ends of the ranges. In the case of *N*-aroyloxy-*N*-alkoxyamides (**9**, R″ = aryl) the amide carbonyl absorption is strongly sensitive to *para* substituents on the ester group.[30,34] The carbonyls of **17** and **18** are typical of *N*-aroyloxy-*N*-alkoxyamides (**9**, R″ = aryl) and the difference, albeit small, can be accounted for on the basis of the strong $+I$ effect of the *tert*-butyl group on the ester group of **18**.

The vibrational frequencies of *N*-acyloxy-*N*-alkoxyamides, **9**, including **17** and **18**, correspond to that observed for the twisted 1-aza-2-adamantanone **14**.[8,9] In all cases where the nitrogen lone pair, either through twisting/pyramidalisation or pyramidalisation alone (anomeric amides), loses conjugation with the carbonyl, the configuration is analogous to an ester rather than a ketone. As with esters and acid halides,[55,56] the carbonyl stretch frequency is higher than ketones and aldehydes on account of destabilisation of the polar form of the carbonyl by the $-I$ effect of the nitrogen (Fig. 6).

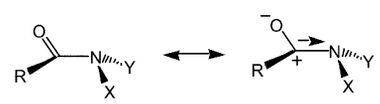

Fig. 6 Inductive destabilisation of the polar form of anomeric amide carbonyls.

The ^{13}C NMR amide $^{13}C=O$ resonances for **17** and **18** are affected in a predictable manner and support this assertion. Both are in a similar region to ester carbonyl carbons (typically 164–176 ppm). While chemical shifts in *N*-acetoxy-*N*-alkoxyamides (**9**) [174.1 ppm benzamides, 176.5 ppm acetamides] are uniformly shifted to higher frequency by about 8 ppm relative to their precursor hydroxamic esters,[27,31,34] they are not ketonic and appear some 20 ppm upfield of aryl/alkyl ketones. The shift in the "most twisted" amide **14** is at a significantly higher

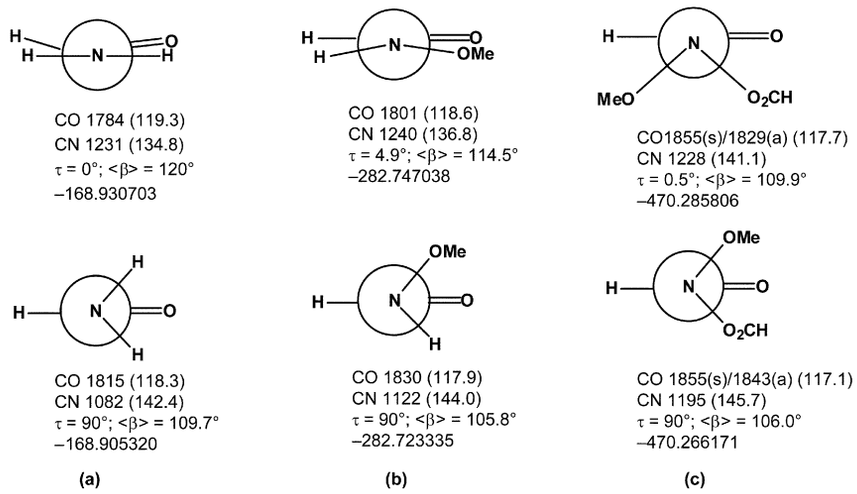

Fig. 7 Carbonyl and *C–N* vibrational frequencies (cm^{-1}) and bond lengths (pm; in parentheses), twist angles (τ), average angles at nitrogen <β> and energies (hartrees) computed at HF/6-31G* level for ground state and orthogonal conformations of (a) formamide, (b) *N*-methoxyformamide and (c) *N*-formyloxy-*N*-methoxyformamide (**5**).

frequency (200 ppm) and has been labelled as aldehydic by Kirby and coworkers.[10] However, rigid bicyclic ketones exhibit much higher carbonyl ^{13}C NMR shifts and 200 ppm represents a shift to higher field of similar magnitude relative to 2-adamantanone which has a carbonyl ^{13}C NMR resonance at 218 ppm.

The mutagens **17** and **18** have small twist angles (Table 1). However, the lone pair in these and other *N*-acyloxy-*N*-alkoxyamides is essentially non-conjugated even though its axis lies close to a plane containing the carbon p-orbital. Gas-phase vibrational frequencies can be computed with some accuracy using molecular orbital methods,[57,58] which can also provide structural data about transition states or unstable conformations. Using HF/6-31G* optimised geometries, we have calculated the gas phase carbonyl and *C–N* stretch frequencies for ground-state and fully twisted conformations of formamide (Fig. 7a), *N*-methoxyformamide (Fig. 7b) and *N*-formyloxy-*N*-methoxyformamide (**5**) (Fig. 7c). Fully twisted formamide and *N*-methoxyformamide have carbonyl stretch frequencies that are ~30 cm^{-1} higher than the planar or near-planar ground state structures indicating a significant loss of resonance in the twisted forms. The *C–N* stretch frequencies are reduced by 149 and 119 cm^{-1} respectively. The carbonyl vibrational frequencies for twisted *N*-formyloxy-*N*-methoxyformamide (**5**) are strongly coupled but both the symmetrical and asymmetrical stretch frequencies are very similar to those of the ground state conformation (Fig. 7c). In this case, the *C–N* stretch frequency is reduced by only 48 cm^{-1}. Thus, when compared to formamide or *N*-methoxyformamide, both the carbonyl stretch and the *C–N* bond stretch frequencies are much less sensitive to the orientation of the sp^3 lone pair. Changes in the frequencies and bond lengths upon twisting the lone pair of *N*-formyloxy-*N*-methoxyformamide out of conjugation (Fig. 7c) would suggest that, at HF/6-31G* level in the gas phase at least, some residual pi overlap is lost. The calculated variations in *C=O* and *C–N* vibrational frequencies for formamide (+31 and −149 cm^{-1} respectively) upon twisting the lone pair into the *OCN* plane are in accordance with changes in bond lengths (−1 and +7.6 pm respectively) and reflect the contemporary view that pi donation to the carbonyl carbon in the planar form does not result in an equivalent loss in *C=O* pi-bond character.[1] Similar results are found for *N*-methoxyformamide.

Conformation and anomeric effects

Calculations on various bisheteroatom-substituted amides provided evidence for operation of anomeric interactions through the amide nitrogen.[36,37,59] In addition, dynamic NMR studies on hydrazines **7** yielded *N–N* rotational barriers of between 65 and 72 kJ mol^{-1} which is indicative of substantial n_N–σ^*_{NOR} overlap and accordingly, the *N–N* bond in the crystal structure of **13** was only 138.9 pm.[35] In *N*-acyloxy-*N*-alkoxyamides **17** and **18**, such negative hyperconjugation would be expected in the direction n_O–σ^*_{NOAcyl} as opposed to n_{OAcyl}–σ^*_{NOR} and pBP/DN*//6-31G* calculations on **5** confirmed this; the p-type lone pair on the methoxyl oxygen was collinear with the *N–OCHO* bond.[50] X-ray data for **17** and **18** provides structural evidence for a n_O–σ^*_{NOAcyl} anomeric interaction. The dihedrals C(14)O(3)N(1)-O(1) for **17** and C(18)O(3)N(1)O(1) for **18** were 96.7 and 96.2° respectively, which is almost ideal for an n_O–σ^*_{NOAcyl} overlap, whereas dihedrals C(7)O(1)N(1)O(3) in **17** (−137.6°) and **18** (−141.6) would indicate a poor n_{OAcyl}–σ^*_{NOR} interaction. As a consequence, *N–OR* bonds should be shorter than normal. A comparison between *N–OR* bond lengths of **17** and **18** with those of the parent hydroxamic esters is inappropriate on account of differences in hybridisation at nitrogen (in hydroxamic esters, nitrogen is largely sp^2 hybridised leading naturally to shorter *N–O* bonds). However, a comparison can be made with hydroxylamines since the nitrogen is fully tetrahedral in these, as well as in *N*-acyloxy-*N*-alkoxyamides (**9**). Typically, the *N–O* bond in hydroxylamines is of the order of 144–146 pm. Values in this range have also been computed for fully twisted hydroxamic esters where the nitrogen also assumes a pyramidal geometry.[36] The r_{NOR} distances of 140.17 pm and 140.14 pm in **17** and **18** respectively represent very significant shortening, presumably through an effective n_O–σ^*_{NOAc} anomeric interaction.

The solid-state structure of both molecules indicates a degree of interaction between the benzyloxy and benzoyloxy substituents, which is most probably brought about by several factors including desolvation, an electrostatic pi–pi stacking interaction and CH/π interactions. The ester carbonyl C(7), with the normal positive electrostatic potential over the carbon, is 322 and 332 pm from C(13) in **17** and C(17) in **18**, respectively, which is ideal for a pi–pi stacking interaction with the benzyloxy ring which has a negative electrostatic potential.[60] In addition, both benzyloxy *tert*-butyls have C–H bonds pointing towards the ester aryl pi-cloud. A C(18)–H in **17** points directly at C(4) (C(18)–C(4) = 396 pm) while in **18**, a C(20)–H points directly at C(5) (C(20)–C(5) = 420 pm). Nishio and coworkers have shown that such interactions can affect conformation in crystal structures although the distances are larger for the interactions in **17** and **18** than the D_{max} chosen in their study (305 ppm).[61] Recently, Tsuzuki *et. al.* have computed much longer C–C distances for optimum CH/π interactions (380–400 pm).[62]

The conformations in the solid state are not expected in solution. Although the ^{1}H NMR resonances of the three *tert*-butyl groups in **18** are very similar (δ_H 1.29, 1.33 and 1.35) careful analysis enabled assignment of the upfield singlet to the benzyloxy *tert*-butyl group. A NOESY spectrum failed to detect any correlations between these protons and those at C(5) or C(6) on the benzoyloxy side chain. In addition, the chemical shifts of the benzyloxy aryl protons in **18** (singlet at δ 7.34) and 4-*tert*-butylbenzyloxy-4-*tert*-butylbenzamide **16** (AB system at δ 7.42 are very similar suggesting that in **18** they are not under the influence of the anisotropy of the 4-*tert*-butylbenzoyloxy substituent. We conclude from this that conformations similar to those shown in Figs. 2 and 3 are likely to be minor contributors in the solution state. Interestingly, the AM1 optimised geometry of **17** (Fig. 8) satisfactorily reproduces the unique properties of this *ONO* system but the benzyloxy and benzoyloxy groups are rotated away from each other in a conformation that is significantly lower in energy in the gas phase than the single point energy computed for the conformation in the crystal structure.

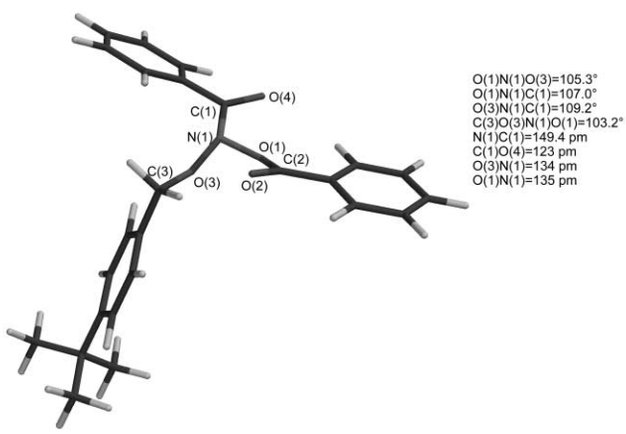

Fig. 8 AM1 optimised geometry of *N*-benzoyloxy-*N*-(4-*tert*-butylbenzyloxy)benzamide (**17**).

Both **17** and **18** have recently been subjected to the Ames *Salmonella* assay by which we determine relative mutagenicities for these direct-acting mutagens.[63] While **17**, with a single benzyloxy *tert*-butyl group, exhibits mutagenic activity that is largely in keeping with its hydrophobicity and reactivity, moderated slightly by the steric influence of the *tert*-butyl group, the tri-*tert*-butylated substrate, **18**, was found to be completely inactive.‡ In a future publication we will report that *N*-benzoyloxy-*N*-benzyloxybenzamides with one *para tert*-butyl group (on any of the three side chains) are appreciably mutagenic but the same tri-arylated substrate with two or three *para tert*-butyl groups are essentially non-mutagenic. We attribute this difference to a severe impediment to binding in the major and minor grooves of DNA with the bulkier substrates. These differences in mutagenicity would imply that the conformation in the crystal structures of **17** and **18** is unlikely to reflect their behaviour in solution, or in association with DNA, since the spatial requirements of both molecules, as depicted in Figs. 2 and 3 are very similar.

Experimental

Melting points were determined on a Reichert Microscopic Hot-Stage and are uncorrected. Infrared spectra were recorded on a Perkin-Elmer 1725X Fourier-transform instrument. 300 MHz ^{1}H and 75 MHz ^{13}C NMR spectra were recorded on a Bruker Avance 300 FT spectrometer. Deuterated chloroform ($CDCl_3$) was commercially obtained from Aldrich. All routine samples for structural analysis were run at 300 K in $CDCl_3$, with tetramethylsilane (0.1%) or $CHCl_3$ as an internal standard. Chemical shifts are reported in ppm down field of TMS. Abbreviations used to indicate spectral multiplicity are: s (singlet), d (doublet), t (triplet), q (quartet), m (multiplet). Preparative plate chromatography was carried out centrifugally on a Harrison 7924T Research Chromatotron. Microanalyses were performed at the Microanalytical Unit, Research School of Chemistry, Australian National University. Electrospray mass spectral data was obtained on a Varian 1200L spectrometer.

Computational methods

Molecular orbital calculations were executed with MACSPARTAN PRO and SPARTAN 5 molecular modelling software.[64,65] Geometries were optimised at the HF/6-31G* level of theory. Frequency calculations at the HF/6-31G* level were carried out to verify stationary points as minima (all real frequencies) and transition states (exactly one imaginary frequency) and to determine gas phase carbonyl and *C–N* stretch frequencies in ground state and twisted conformations of formamide, *N*-methoxyformamide and *N*-formyloxy-*N*-methoxyformamide.

Syntheses

The synthesis of *N*-(4-*tert*-butylbenzyloxy)benzamide (**15**) and 4-*tert*-butylbenzyl bromide, potassium 4-(*tert*-butyl)benzohydroxamate[27] and sodium 4-*tert*-butylbenzoate have been described previously.[30]

General synthesis of alkyl substituted benzohydroxamates.[66] The appropriate benzohydroxamic ester was synthesised in good yield by the reaction of the potassium salt with the relevant alkyl bromide and a 10% excess of sodium carbonate in a 50% aqueous solution of methanol.

***N*-(4-*tert*-Butylbenzyloxy)-4-*tert*-butylbenzamide 16.** Potassium 4-(*tert*-butyl)benzohydroxamate and 4-*tert*-butylbenzyl bromide were reacted in the presence of a 10% excess of sodium carbonate in a 50% aqueous solution of methanol. Crystallisation from benzene–petroleum spirit, afforded 4-*tert*-butylbenzyloxy-4-*tert*-butylbenzamide in 57% yield. Mp 179–181 °C, (Found: C, 77.84; H, 8.66; N, 4.04%. $C_{22}H_{29}NO_2$ requires C, 77.84; H, 8.61, N, 4.13%); ν_{max} ($CHCl_3$) 3300 (N–H) and 1679 cm^{-1} (C=O); δ_H(300 MHz, $CDCl_3$) 1.34 (9H, s, C[CH_3]$_3$), 1.35 (9H, s, C[CH_3]$_3$), 5.03 (2H, s, OCH_2Ar), 7.40 (6H, m, Ar*H*), and 7.63 (2H, d, *o*-*ArH*–CO). δ_C(75 MHz, $CDCl_3$) 31.1 (q, Ar–C[CH_3]$_3$), 31.3 (q, Ar–C[CH_3]$_3$) 34.7 (s, Ar–*C*[CH$_3$]$_3$), 35.0 (s, Ar–*C*[CH$_3$]$_3$), 76.6 (t, OCH_2Ar), 125.3 (d, *m*-*ArC*-*t*Bu), 125.4 (d, *m*′-*ArC*–tBu), 126.9 (d, *o*′-*ArC*), 129.2 (d, *o*-ArC), 130.4 (s, *ArC*–CO), 137.8 (s, OCH$_2$–*ArC*), 146.0 (s, *ArC*–C[CH$_3$]$_3$), 150.5 (s, *ArC*–C[CH$_3$]$_3$), and 166.3 (s, Ar–*C*O–NH); *m*/*z* (ESI) 362 [M + Na$^+$].

General synthesis of *N*-benzyloxy-*N*-chlorobenzamides. A solution of the appropriate *N*-benzyloxybenzamide and a 2–3 molar excess of *tert*-butyl hypochlorite in CH_2Cl_2 was stirred in the dark under anhydrous conditions for 3–6 hours. The progress of the reaction was monitored by thin-layer chromatography until complete, at which time the solvent and excess *tert*-butyl hypochlorite were removed in the dark under reduced pressure at 30 °C to afford the *N*-chlorohydroxamic ester in excellent yield (90–100%). The *N*-chlorohydroxamic esters were used without further purification.

***N*-(4-*tert*-Butylbenzyloxy)-*N*-chlorobenzamide.** *N*-4-*tert*-butylbenzyloxy-*N*-chlorobenzamide was produced quantitatively as a yellow oil. ν_{max} ($CHCl_3$) 1709 (C=O) cm^{-1}; δ_H(300 MHz, $CDCl_3$) 1.36 (9H, s, C[CH_3]$_3$), 5.11 (2H, s, OCH_2Ar), 7.24

‡ For **17**, Log (TA100/1 μmol plate^{-1}) = 3.05; for **18**, Log (TA100/1 μmol plate^{-1}) = 2.5 (background reversion rate).

(2H, t, *m*-Ar*H*), 7.42 (4H, m, Ar*H*), 7.57 (1H, t, *p*-Ar*H*), and 7.73 (2H, d, *o*-ArH).

***N*-(4-*tert*-Butylbenzyloxy)-*N*-chloro-4-*tert*-butylbenzamide.** *N*-4-*tert*-butylbenzyloxy-*N*-chloro-4-*tert*-butylbenzamide was prepared in 89% yield and was a yellow oil,. ν_{max} ($CHCl_3$) 1693 (C=O) cm^{-1}; δ_H(300 MHz, $CDCl_3$) 1.32 (9H, s, C[CH_3]$_3$), 1.36 (9H, s, C[CH_3]$_3$), 5.08 (2H, s, OCH_2Ar), 7.21 (2H, d, Ar*H*), 7.36 (2H, d, Ar*H*), 7.43 (2H, d, *m*-*ArH*–CO), and 7.67(2H, d, *o*-*ArH*–CO).

General synthesis of *N*-acyloxy-*N*-alkoxyamides. *N*-Benzyloxy-*N*-chlorobenzamides were benzoyloxylated by treatment with 1.4 molar equivalents of the appropriate sodium benzoate in dry acetone, at room temperature, for 12–72 hours in the dark. The reaction was monitored by thin-layer chromatography. Filtration and concentration under reduced pressure provided the *N*-benzoyloxyl derivatives in good yields. Products were either obtained in a pure state or were further purified by centrifugal chromatography (15% ethyl acetate: 85% petroleum spirit or 10% ethyl acetate–90% petroleum spirit). In all cases, mutagens were characterised spectroscopically (^{1}H and ^{13}C NMR chemical shift assignments for the benzyloxy and benzoyloxy side chains are indicated by the ″′″ and ″*″ symbols respectively).

***N*-Benzoyloxy-*N*-(4-*tert*-butylbenzyloxy)benzamide (17).** Purification by centrifugal chromatography (15% ethyl acetate–85% petroleum spirit) provided the title compound as a colourless prismatic solid (86% yield). Recrystallisation from ethyl acetate–petroleum spirit afforded prisms mp 87–89 °C. ν_{max} ($CHCl_3$) 1758 (ester CO stretch), 1728 (amide CO stretch) cm^{-1}; δ_H(300 MHz, $CDCl_3$) 1.30 (9H, s, C[CH_3]$_3$), 5.26 (2H, s, OCH_2Ar), 7.35 (4H, s, *o*′, *m*′-ArH), 7.43 (4H, *m*- and *m**-ArH), 7.54 (1H, t, *p*-Ar*H*), 7.61 (1H, t, *p**-Ar*H*), 7.83 (2H, d, *o*-Ar*H*), and 7.98 (2H, d, *o**-Ar*H*). δ_C(75 MHz, $CDCl_3$) 31.1 (q, Ar–C[*C*H$_3$]$_3$, 34.6 (s, Ar–*C*[CH$_3$]$_3$), 77.4 (t, O*C*H$_2$Ar), 125.4 (d, *m*′-Ar*C*-*t*Bu), 126.9 (d, *o*′-Ar*C*–*t*Bu), 127.4 (d, *o*-Ar*C*), 128.3 (d, *m**-Ar*C*), 128.6 (d, *m*-Ar*C*), 129.2 (d, *o**-Ar*C*), 130.0 (s, *C**–C(O)ON), 131.7 (d, *p*-Ar*C*), 132.7 (s, Ar*C*–C(O)N), 133.9 (d, *p**-Ar*C*), 134.5 (s, OCH$_2$–Ar*C*) 151.8 (s, *Ar*C–C[CH$_3$]$_3$), 164.2 (s, O*C**OAr), and 174.4 (s, Ar–*C*O–NH); *m*/*z* (ESI) 426 [M + Na^+].

***N*-(4-*tert*-Butylbenzoyloxy)-*N*-(4-*tert*-butylbenzyloxy)-4-*tert*-butylbenzamide 18.** Purification by centrifugal chromatography (15% ethyl acetate–85% petroleum spirit) provided this compound as a white solid in 79% yield. Crystallisation from ethyl acetate–petroleum spirit afforded prisms, mp 148–150 °C (Found: C, 77.18; H, 8.26; N, 2.45% $C_{22}H_{29}NO_2$ requires C, 76.86; H, 8.01, N, 2.72%). ν_{max} ($CHCl_3$) 1754 (ester CO stretch), 1726 (amide CO stretch) cm^{-1}; δ_H(300 MHz, $CDCl_3$) 1.29 (9H, s, C[*CH*′$_3$]$_3$), 1.33 (9H, s, C[*CH*$_3$]$_3$), 1.35 (9H, s, C [*CH**$_3$]$_3$), 5.26 (2H, s, O*CH*′$_2$Ar), 7.35 (4H, s, *o*′,*m*′-Ar*H*–*t*Bu), 7.42 (2H, d, *m*-Ar*H*), 7.45 (2H, d, *m**-Ar*H*), 7.79 (2H, d, *o*-Ar*H*), and 7.91 (2H, d, *o**-Ar*H*). δ_C(75 MHz, $CDCl_3$) 31.2 (2 × q, Ar–C[*C*H$_3$]$_3$, Ar–C[*C**H$_3$]$_3$), 31.4 (q, ArC′[*C*H$_3$]$_3$), 34.6 (s, Ar–*C*′[CH$_3$]$_3$), 35.1 (s, Ar–*C*[CH$_3$]$_3$), 35.2(s, Ar–*C**[CH$_3$]$_3$), 76.6 (t, O*C*′H$_2$Ar), 125.0 (d, *m*-Ar*C*), 125.2 (d, *m*′-Ar*C*), 125.2 (d, *m**-ArC), 125.7 (s, Ar*C**–C(O)ON), 128.9 (d, *o*′-Ar*C*–CH$_2$ON), 129.1 (d, *o*-Ar*C*–C(O)N), 129.8 (d, *o**-Ar*C*–C(O)ON), 128.7 (s, Ar*C*–C(O)N), 132.0 (s, Ar*C*′–CH$_2$ON), 151.7 (s, Ar*C*′-*t*Bu), 156.5 (s, Ar*C*–*t*Bu), 157.7 (s, *p**-Ar*C*), 164.3 (s, O*C**(O)Ar) and 174.5. (s, Ar–*C*(O)N); *m*/*z* (ESI) 538 [M + Na^+].

X-Ray crystallography.§ Colourless prismatic crystals were attached with Exxon Paratone N, to a short length of fibre supported on a thin piece of copper wire inserted in a copper mounting pin. The crystals were quenched at at 150(2) Kelvin in a cold nitrogen gas stream from an Oxford Cryosystems Cryostream. A Bruker SMART 1000 CCD diffractometer employing graphite monochromated MoKα radiation generated from a sealed tube was used for the data collection, and data were collected with ω scans to 0.75 Å. The data integration and reduction were undertaken with SAINT and XPREP,[67] and subsequent computations were carried out with the teXsan[68] WinGX,[69] XSHELL[70] and XTAL[71] graphical user interfaces. The structures were solved by direct methods with SIR97,[72] and extended and refined with SHELXL-97.[73] The non-hydrogen atoms were modelled with anisotropic displacement parameters, and a riding atom model with group displacement parameters was used for the hydrogen atoms. ORTEP[52] depictions of the molecules with 20% displacement ellipsoids are provided in Figs. 2 and 3.

Crystal data for (17). Formula $C_{25}H_{25}NO_4$, *M* 403.46, monoclinic, space group $P2_1/c$(#14), *a* 9.974(3), *b* 14.182(5), *c* 16.104(5) Å, *β* 107.088(5)°, *V* 2177.4(12) Å^3, D_c 1.231 g cm^{-3}, *Z* 4, crystal size 0.445 by 0.310 by 0.244 mm, colour: colourless, habit prismatic μ(MoKα) 0.083 cm^{-1}, *T*(Gaussian[67,68] [Bruker, 1995 #709;1997–1998 #710])$_{min,max}$ 0.963, 0.979, $2\theta_{max}$ 56.46, *hkl* range −13 12, −18 18, −20 20, *N* 18940, N_{ind} 5007(R_{merge} 0.0274), N_{obs} 4069($I > 2\sigma(I)$), N_{var} 274, residuals¶ *R*1(*F*) 0.0349, *wR*2(F^2) 0.0951, GoF(all) 1.465, $\Delta\rho_{min,max}$ −0.203, 0.222 e^- Å^{-3}.

Crystal data for (18). Formula $C_{33}H_{41}NO_4$, *M* 515.67, monoclinic, space group $P2_1/n$(#14), *a* 9.2910(19), *b* 17.063(4), *c* 18.640(4) Å, *β* 98.007(4)°, *V* 2926.2(11) Å^3, D_c 1.171 g cm^{-3}, *Z* 4, crystal size 0.465 by 0.174 by 0.173 mm, colour: colourless, habit prism, μ(MoKα) 0.076 mm^{-1}, $2\theta_{max}$ 56.56, *hkl* range −12 12, −22 22, −24 24, *N* 29776, N_{ind} 7092(R_{merge} 0.0300), N_{obs} 5242($I > 2\sigma(I)$), N_{var} 352, residuals‖ *R*1(*F*) 0.0425, *wR*2(F^2) 0.0909, GoF(all) 1.318, $\Delta\rho_{min,max}$ −0.260, 0.238 e^- Å^{-3}.

Acknowledgements

The authors are grateful to the Australian Research Council for financial support and to the Canadian Rotary Exchange Fellowship scheme for a scholarship to Ashley-Mae Gillson.

§ CCDC reference numbers 212185 (**17**) and 212186 (**18**). See http://www.rsc.org/suppdata/ob/b3/b306098p/ for crystallographic data in .cif or other electronic format.

¶ $R1 = \Sigma||F_o| - |F_c||/\Sigma|F_o|$ for $F_o > 2\sigma(F_o)$; $wR2 = (\Sigma w(F_o^2 - F_c^2)^2/\Sigma(wF_c^2)^2)^{1/2}$ all reflections; $w = 1/[\sigma^2(F_o^2) + (0.0400P)^2]$ where $P = (F_o^2 + 2F_c^2)/3$

‖ $R1 = \Sigma||F_o| - |F_c||/\Sigma|F_o|$ for $F_o > 2\sigma(F_o)$; $wR2 = (\Sigma w(F_o^2 - F_c^2)^2/\Sigma(wF_c^2)^2)^{1/2}$ all reflections; $w = 1/[\sigma^2(F_o^2) + (0.02P)^2 + 0.5P]$ where $P = (F_o^2 + 2F_c^2)/3$

References

1 K. B. Wiberg, in *Origin of the Amide Rotational Barrier*, ed. A. Greenberg, C. M. Breneman and J. F. Liebman, John Wiley & Sons, Inc., New York, 2000.
2 E. L. Eliel, S. H. Wilen and L. N. Mander, *Stereochemistry of Organic Compounds*, John Wiley & Sons, Inc., New York, 1994.
3 J. Sandström, *Dynamic NMR Spectroscopy*, Academic Press, London, 1982.
4 A. Greenberg, C. Breneman and J. F. Liebman, *The Amide Linkage: Structural Significance in Chemistry, Biochemistry and Material Science*, Wiley, New York, 2000.
5 S. Yamada, N. Nunami and K. Hori, *Chem. Lett.*, 1998, 451.
6 S. Yamada, *Rev. Heteroat. Chem.*, 1999, **19**, 203.
7 S. Yamada and A. Homma, *Chem. Commun.*, 2002, 2656.
8 A. J. Kirby, I. V. Komarov, P. D. Wothers and N. Feeder, *Angew. Chem., Int. Ed.*, 1998, **37**, 785.
9 A. J. Kirby, I. V. Komarov, K. Kowski and P. Rademacher, *J. Chem. Soc., Perkin Trans. 2*, 1999, 1313.
10 A. J. Kirby, I. V. Komarov and N. Feeder, *J. Chem. Soc., Perkin Trans. 2*, 2001, 522.
11 C. N. Cow, J. F. Britten and P. H. M. Harrison, *Chem. Commun.*, 1998, 1147.
12 P. A. Duspara, C. F. Matta, S. I. Jenkins and P. H. M. Harrison, *Org. Lett.*, 2001, **3**, 495.

13 T. Ohwada, T. Achiwa, I. Okamoto, K. Shudo and K. Yamaguchi, *Tetrahedron Lett.*, 1998, **39**, 865.
14 T. Ohwada, *Yakugaku Zasshi*, 2001, **121**, 65.
15 S. Sun, L. Edwards and P. Harrison, *J. Chem. Soc., Perkin Trans. 2*, 1998, 437.
16 S. Yamada and H. Katsumata, *J. Org. Chem.*, 1999, **64**, 9365.
17 A. Greenberg and T. D. DuBois, *J. Mol. Struct.*, 2001, **567**, 303.
18 C. G. Bashore, I. J. Samardjiev, J. Bordner and J. W. Coe, *J. Am. Chem. Soc.*, 2003, **125**, 3268.
19 F. K. Winkler and J. D. Dunitz, *J. Mol. Biol.*, 1971, **59**, 169.
20 G. Yamamoto, N. Tsubai, H. Murakami and Y. Mazaki, *Chem. Lett.*, 1997, 1295.
21 G. Yamamoto, F. Nakajo, N. Tsubai, H. Murakami and Y. Mazaki, *Bull. Chem. Soc. Jpn.*, 1999, **72**, 2315.
22 S. A. Glover, A. Goosen, C. W. McCleland and J. L. Schoonraad, *J. Chem. Soc., Perkin Trans. 2*, 1984, 2255.
23 S. A. Glover, A. Goosen, C. W. McCleland and J. L. Schoonraad, *Tetrahedron*, 1987, **43**, 2577.
24 S. A. Glover, C. A. Rowbottom, A. P. Scott and J. L. Schoonraad, *Tetrahedron*, 1990, **46**, 7247.
25 R. G. Gerdes, S. A. Glover, J. F. Ten Have and C. A. Rowbottom, *Tetrahedron Lett.*, 1989, **30**, 2649.
26 J. J. Campbell, S. A. Glover and C. A. Rowbottom, *Tetrahedron Lett.*, 1990, **31**, 5377.
27 J. J. Campbell, S. A. Glover, G. P. Hammond and C. A. Rowbottom, *J. Chem. Soc., Perkin Trans. 2*, 1991, 2067.
28 J. J. Campbell and S. A. Glover, *J. Chem. Soc., Perkin Trans. 2*, 1992, 1661.
29 A. M. Bonin, S. A. Glover and G. P. Hammond, *J. Chem. Soc., Perkin Trans. 2*, 1994, 1173.
30 A. M. Bonin, S. A. Glover and G. P. Hammond, *J. Org. Chem.*, 1998, **63**, 9684.
31 J. J. Campbell and S. A. Glover, *J. Chem. Res. (S)*, 1999, **8**, 474; J. J. Campbell and S. A. Glover, *J. Chem. Res. (M)*, 1999, 2075.
32 T. M. Banks A. M. Bonin, J. J. Campbell, S. A. Glover, G. P. Hammond, A. S. Prakash and C. A. Rowbottom, *Mutat. Res.*, 2001, **494/1-2**, 115.
33 T. M. Banks, A. M. Bonin, S. A. Glover and A. S. Prakash, *Org. Biomol. Chem.*, 2003, **1**, 2238.
34 S. A. Glover, *Tetrahedron*, 1998, **54**, 7229.
35 S. A. Glover, G. Mo, A. Rauk, D. Tucker and P. Turner, *J. Chem. Soc., Perkin Trans. 2*, 1999, 2053.
36 S. A. Glover and A. Rauk, *J. Org. Chem.*, 1996, **61**, 2337.
37 S. A. Glover and A. Rauk, *J. Org. Chem.*, 1999, **64**, 2340.
38 S. A. Glover and A. Rauk, *J. Chem. Soc., Perkin Trans. 2*, 2002, 1740.
39 R. O. C. Norman, R. Purchase and C. B. Thomas, *J. Chem. Soc., Perkin Trans. 1*, 1972, 1701.
40 R. J. Crawford and R. Raap, *J. Org. Chem.*, 1963, **28**, 2419.
41 J. H. Cooley, M. W. Mosher and M. A. Khan, *J. Am. Chem. Soc.*, 1968, **90**, 1867.
42 J. H. Cooley, D. H. Stone and H. Oguri, *J. Am. Chem. Soc.*, 1977, **42**, 3096.
43 Y. Kikugawa and M. Kawase, *J. Am. Chem. Soc.*, 1984, **106**, 5728.
44 Y. Kikugawa and M. Shimada, *Chem. Lett.*, 1987, 1771.
45 M. Kawase, T. Kitamura and Y. Kikugawa, *J. Org. Chem.*, 1989, **54**, 3394.
46 J. M. Buccigross, S. A. Glover and G. P. Hammond, *Aust. J. Chem.*, 1995, **48**, 353.
47 S. A. Glover, G. Mo and A. Rauk, *Tetrahedron*, 1999, **55**, 3413.
48 M. Adams, S. A. Glover and D. J. Tucker, 2001, unpublished results.
49 S. A. Glover and G. Mo, *J. Chem. Soc., Perkin Trans. 2*, 2002, 1728.
50 S. A. Glover, *Arkivok*, 2001. Issue in Honour of Prof. O. S. Tee, ms. OT-308C (http://www.arkat-usa.org/ark/journal/Volume2/Part3/Tee/OT-308C/OT-308.htm).
51 A. J. Kirby, I. V. Komarov and N. Feeder, *J. Am. Chem. Soc.*, 1998, **120**, 7101.
52 C. K. Johnson, ORTEP-II: A FORTRAN Thermal Ellipsoid Plot Program for Crystal Structure Illustrations, Report ORNL-5138, Oak Ridge National Laboratory, Oak Ridge, TN, USA, 1976.
53 J. D. Dunitz, *X-Ray Analysis and Structure of Organic Molecules*, Cornell University Press, London, 1979.
54 F. H. Allen, *Acta Crystallogr., Sect. B: Struct. Sci.*, 2002, **58**, 380.
55 L. J. Bellamy, *Advances in Infrared Group Frequencies*, Methuan and Co. Ltd., Bungay, 1968.
56 L. J. Bellamy, *The Infra-red Spectra of Complex Molecules*, Chapman and Hall, London, 1975.
57 W. J. Hehre, L. Radom, P. v. R. Schleyer and J. A. Pople, *Ab Initio Molecular Orbital Theory*, John Wiley and Sons, New York, 1986.
58 A. P. Scott and L. Radom, *J. Phys. Chem.*, 1996, **100**, 16502.
59 J. M. Buccigross and S. A. Glover, *J. Chem. Soc., Perkin Trans. 2*, 1995, 595.
60 C. A. Hunter, K. R. Lawson, J. Perkins and C. J. Urch, *J. Chem. Soc., Perkin Trans. 2*, 2001, 651.
61 Y. Umezawa, S. Tsuboyama, H. Takahashi, J. Uzawa and M. Nishio, *Tetrahedron*, 1999, **55**, 10047.
62 S. Tsuzuki, K. Honda, T. Uchimaru, M. Mikami and K. Tanabe, *J. Am. Chem. Soc.*, 2000, **122**, 3746.
63 A. M. Bonin, A.-M. E. Gillson and S. A. Glover, unpublished results.
64 MacSpartan *Pro* Version 1, Wavefunction, Inc., 18401 Van Karman, Suite 370, Irvine, California, 92612.
65 Spartan Version 5, Wavefunction, Inc., 18401 Van Karman, Suite 370, Irvine, California, 92612.
66 J. H. Cooley, W. D. Bills and J. R. Throckmorton, *J. Org. Chem.*, 1960, **25**, 1734.
67 Bruker, SMART, SAINT and XPREP. Area detector control and data integration and reduction software, Bruker Analytical X-ray Instruments Inc., 1995, Madison, Wisconsin, USA.
68 teXsan for Windows: Single Crystal Structure Analysis Software, Molecular Structure Corporation, 1997–1998, 3200 Research Forest Drive, The Woodlands, TX 77381, USA.
69 L. J. Farrugia, *J. Appl. Crystallogr.*, 1999, **32**, 837.
70 *XSHELL. Graphical interface for crystal structure refinement*, Bruker Analytical X-ray Instruments Inc., 1995, Madison, Wisconsin, USA.
71 S. R. Hall, D. J. du Boulay and R. Olthof-Hazekamp, *Eds. Xtal3.6 System*, University of Western Australia, 1999.
72 A. Altomare, M. Cascarano, C. Giacovazzo and A. Guagliardi, *J. Appl. Crystallogr.*, 1993, **26**, 343.
73 G. M. Sheldrick, SHELXL-97, Program for refinement of crystal structures, University of Göttingen, Germany, 1997.